THE ASTROPHYSICAL JOURNAL, 404:L83–L86, 1993 February 20

EFFECTS OF MAGNETIC FIELDS AND ROTATION ON THE FRAGMENTATION OF FILAMENTARY MOLECULAR CLOUDS: COMPARISON OF THE THEORY WITH THE ORION A CLOUD

TOMOYUKI HANAWA,[1] FUMITAKA NAKAMURA,[1] TOMOAKI MATSUMOTO,[1] TAKENORI NAKANO,[2]
KEN'ICHI TATEMATSU,[2] TOMOFUMI UMEMOTO,[2] OSAMU KAMEYA,[3] NAOMI HIRANO,[4]
TETSUO HASEGAWA,[5] NORIO KAIFU,[6] AND SATOSHI YAMAMOTO[1]

Received 1992 June 29; accepted 1992 December 3

ABSTRACT

We discuss the fragmentation of a filamentary molecular cloud on the basis of a magnetohydrodynamical stability analysis and the observations of the Orion A cloud with the Nobeyama 45 m telescope. Our model cloud has axial and helical magnetic fields and rotates around the axis. The dispersion relation for this cloud shows that the presence of a magnetic field and/or rotation shortens the wavelength of the most unstable mode, i.e., the mean distance between the adjacent fragments, measured in units of the filament diameter. We compare the theoretical results with the observed clumpy structure of the filamentary Orion A cloud and find that the sum of magnetic and centrifugal forces in the parent cloud was comparable with the pressure force (thermal and turbulent) and has had significant effects on the fragmentation. The rotation velocity of the filament measured in the ^{13}CO emission line is consistent with this result.

Subject headings: hydromagnetics — instabilities — ISM: individual (Orion Nebula) — ISM: magnetic fields

1. INTRODUCTION

Filamentary features are often found in CO maps of molecular clouds. In these filamentary molecular clouds, we find denser regions called clumps and cores with ^{13}CO, $C^{18}O$, and CS observations. Here we call a 1 pc–sized condensation a *clump* and a 0.1 pc–sized one a *core* for convenience. Clumps are more or less regularly distributed and are likely to be produced from a parent filamentary cloud by fragmentation and contraction. If fragmentation is caused by the self-gravity of the cloud, the distance between the adjacent clumps is of the order of the Jeans length, the characteristic length determined by the self-gravity and the gas pressure (including turbulent pressure), but is modified by the existence of magnetic fields and rotation. Although an isothermal filamentary cloud supported by the pressure alone can take an equilibrium state only for some special line density, or mass per unit length, as long as the surface pressure is negligible (Ostriker 1964), a magnetized and/or rotating filament can take an equilibrium state for any line density exceeding the special line density mentioned above and its diameter depends on the strength of magnetic field and rotation in addition to the self-gravity and the pressure.

Recently some of the present authors have investigated the instability of filamentary molecular clouds taking into account magnetic fields (Nakamura, Hanawa, & Nakano 1992) and rotation (Matsumoto et al. 1993). According to their results, the wavelengths of the most unstable mode, and therefore the mean distance between the adjacent clumps, measured in units of the diameter is shorter, when the magnetic field is stronger and/or the rotation is faster. This effect enables us to estimate the strength of the magnetic field and rotation in a filamentary cloud from the observed ratio of the clump distance to the filament diameter.

The Orion A giant molecular cloud has been investigated extensively by radio and optical observations (see, e.g., the review by Genzel & Stutzki 1989 and the references therein). The L1641 region of this cloud is one of the typical filamentary clouds. The observed line density ($\approx 700\ M_\odot\ pc^{-1}$) and ^{13}CO line width (2–3 km s^{-1}) suggest that the cloud is roughly in virial equilibrium (Tatematsu et al. 1993). The magnetic field in this region manifests itself in the optical polarization (Vrba, Strom, & Strom 1988), the Zeeman effect of the H I emission line (Heiles 1987), and that of the OH absorption line (Troland, Crutcher, & Kazés 1986). Based on these observations Bally (1989) suggested that this cloud is penetrated by a helical magnetic field which is skewed by about 20° from the filament axis. The position-velocity diagrams of the ^{13}CO emission line suggest that this cloud spins around the axis and the centrifugal force supports the cloud at least partly against gravity (Tatematsu et al. 1993; see also Uchida et al. 1991). In addition, the $C^{18}O$ map (Dutrey et al. 1991) and the ^{13}CO map (Bally et al. 1987; Tatematsu et al. 1993) show that several clumps are distributed more or less regularly along this filamentary cloud. By comparing this cloud with the theoretical results, we may be able to estimate the strength of magnetic fields and the degree of rotation.

We describe our model for the filamentary molecular cloud and summarize its stability in § 2. Our model cloud has axial and helical magnetic fields and spins around the axis. The dispersion relation and the wavenumber of the most unstable mode are given as empirical fitting formulae for numerical results. Following a brief summary of the observations, we compare them with the theory in § 3.

[1] Department of Astrophysics, Nagoya University, Chikusa-ku, Nagoya 464-01, Japan.
[2] Nobeyama Radio Observatory, Nobeyama, Minamisaku, Nagano 384-13, Japan.
[3] National Astronomical Observatory, Mizusawa, Iwate 023, Japan.
[4] Laboratory of Astronomy and Geophysics, Hitotsubashi University, Kunitachi, Tokyo 186, Japan.
[5] Institute of Astronomy, University of Tokyo, Mitaka, 181, Japan.
[6] National Astronomical Observatory, Mitaka, 181, Japan.

2. THE MODEL OF A ROTATING MAGNETIZED FILAMENTARY CLOUD

Some of the present authors have recently investigated the linear stability of the filamentary gas cloud taking into account magnetic fields (Nakamura, Hanawa, & Nakano 1992) and rotation (Matsumoto et al. 1992). In their model the distribution in equilibrium of the density, velocity, and magnetic field are expressed in the cylindrical coordinates (r, φ, z) as

$$\rho_0(r) = \rho_c\left(1 + \frac{r^2}{8H^2}\right)^{-2}, \tag{1}$$

$$\boldsymbol{v}_0(r) = (v_r, v_\varphi, v_z) = \left[0, \Omega_c r\left(1 + \frac{r^2}{8H^2}\right)^{-1/2}, 0\right], \tag{2}$$

$$\boldsymbol{B}_0(r) = (B_r, B_\varphi, B_z) = (0, B_\varphi, B_z), \tag{3}$$

$$B_\varphi = B_c \sin\theta \frac{r}{2\sqrt{2}H}\left(1 + \frac{r^2}{8H^2}\right)^{-3/2}, \tag{4}$$

$$B_z = B_c\left(1 + \frac{r^2}{8H^2}\right)^{-3/2}\sqrt{1 + \frac{r^2}{8H^2}\cos^2\theta}, \tag{5}$$

where

$$2(2\pi G\rho_c - \Omega_c^2)H^2 = c_s^2 + \frac{B_c^2}{16\pi\rho_c}(1 + \cos^2\theta). \tag{6}$$

This model has five parameters, ρ_c, c_s, B_c, θ, and Ω_c. The parameter c_s denotes the sound speed of the gas and may include the velocity dispersion of small-scale turbulence. The parameter B_c denotes the strength of magnetic field on the axis $r = 0$ and θ is the pitch angle, $\tan^{-1}(B_\varphi/B_z)$, at $r = \infty$ and characterizes the relative strength of the poloidal and axial magnetic fields. The angular velocity of the gas is nearly constant, $\Omega \simeq \Omega_c$, in the region of $r < 2H$, and the rotation velocity is nearly constant $v_\varphi \simeq 2(2)^{1/2}\Omega_c H$ in the region of $r > 4H$. By adjusting these parameters, this model can mimic a rotating filamentary gas cloud with a helical magnetic field. Since the density distribution given by equation (1) is the same as that of the isothermal filamentary gas clouds investigated by Stodółkiewicz (1963), Ostriker (1964), and Nagasawa (1987) apart from the definition of H, our model is an extension of their models to clouds with nonuniform magnetic field and rotation. Equation (6) can be rewritten as

$$H^2 = \frac{c_s^2}{4\pi G\rho_c}\left(1 + \frac{1 + \cos^2\theta}{2}\alpha + \beta\right), \tag{7}$$

where α and β characterize the effects of magnetic field and rotation, respectively, relative to the gas pressure, and are given by

$$\alpha = \frac{B_c^2}{8\pi\rho_c c_s^2}, \quad \beta = \frac{2\Omega_c^2 H^2}{c_s^2}. \tag{8}$$

On the above equilibrium state is superposed a small perturbation in the form of

$$\rho_1 = \rho_1(r)\exp(-i\omega t + im\varphi + ik_z z). \tag{9}$$

The perturbation equations are solved numerically by a method essentially the same as that of Nakamura, Hanawa, & Nakano (1991). The most unstable mode is an axisymmetric one ($m = 0$) and the approximate dispersion relation for this mode is given by

$$\omega^2 = -4\pi G\rho_c \frac{k_z H}{1 + k_z H}\frac{0.89 + 1.4\alpha}{1 + 1.25\alpha} + c_s^2 k_z^2 \quad (\text{for } \theta = 0). \tag{10}$$

The maximum growth rate obtained from this equation agrees with the numerical results within an error of 5% for $0 \le \alpha \le 10$ and $0 \le \beta \le 10$. The growth rate takes a maximum value at the wavenumber given by

$$k_{z,\max} H = 0.72[(1 + \alpha + \beta)^{1/3} - 0.6] \quad (\text{for } \theta = 0). \tag{11}$$

This empirical formula accounts for our numerical results within an error of 2% in the range of $0 \le \alpha + \beta \le 8$. When $\theta \neq 0$, the growth rate is lower than that for $\theta = 0$ and the wavelength of the most unstable mode is longer. For example, when $\alpha = 1$, the wavelength of the most unstable mode for $\theta = 90°$ is 29% longer than for $\theta = 0°$.

Equation (11) means that the wavelength of the most unstable mode is shorter in units of H when the magnetic field and/or rotation are stronger, or $(\alpha + \beta)$ is larger. Figure 1 (Plate L10) shows the column density distribution of our model clouds suffering from the most unstable mode of perturbation. Figure 1*a* is for $\alpha = \beta = 0$, and Figure 1*b* is for $\alpha = 1$ and $\beta = 0$. The difference between the two cases indicates that we can evaluate the strength of the magnetic field and rotation $(\alpha + \beta)$ from the appearance of fragmentation.

The effective diameter of our model cloud can be defined in the following way. The column density of our model cloud is expressed as

$$\Sigma(r) = \int_{-\infty}^{+\infty}\rho(\sqrt{r^2 + s^2})ds = \sqrt{2}\pi\rho_c H\left(1 + \frac{r^2}{8H^2}\right)^{-3/2}, \tag{12}$$

and decreases to half the maximum at $r = 2.168H$. Accordingly, the FWHM of the integrated intensity of an emission line is equal to $d_{\rm FWHM} = 4.336H$ if the cloud is optically thin. When the cloud is optically thick, FWHM is larger ($d_{\rm FWHM} > 4.336H$) but not by a large factor because $\Sigma(r)$ depends strongly on r.

Substituting $k_{z,\max} = 2\pi/\lambda$ into equation (11), we obtain

$$\alpha + \beta \ge \left[1.75\left(\frac{d_{\rm FWHM}}{\lambda}\right)\left(\frac{d_{\rm FWHM}}{5H}\right)^{-1} + 0.6\right]^3 - 1.0, \tag{13}$$

where λ is the distance between the adjacent fragments formed by the most unstable mode of the gravitational instability and we have normalized $d_{\rm FWHM}$ by $5H$ instead of $4.336H$. The inequality in equation (13) holds for $\theta \neq 0$. With the observed $d_{\rm FWHM}$, the apparent distance between clumps, and the projection angle of the filamentary cloud we can evaluate $\alpha + \beta$ from equation (13).

3. COMPARISON WITH THE ORION A FILAMENTARY CLOUD

Figure 2 (Plate L11) shows the ^{13}CO peak intensity map of the ∫-shaped filament in the Orion A cloud. Examples of the 1 pc–sized clumps are labeled with letters. Although clumps A and B are not clearly separated in the ^{13}CO *peak intensity* map, these clumps are separated more clearly in the ^{13}CO *column density* map of Castets et al. (1990), the C^{18}O integrated intensity map of Dutrey et al. (1991), and the CS (1–0) peak intensity map (Tatematsu et al. 1993).

We evaluated the diameter of the filament by fitting the integrated ^{13}CO intensity map to the model column density

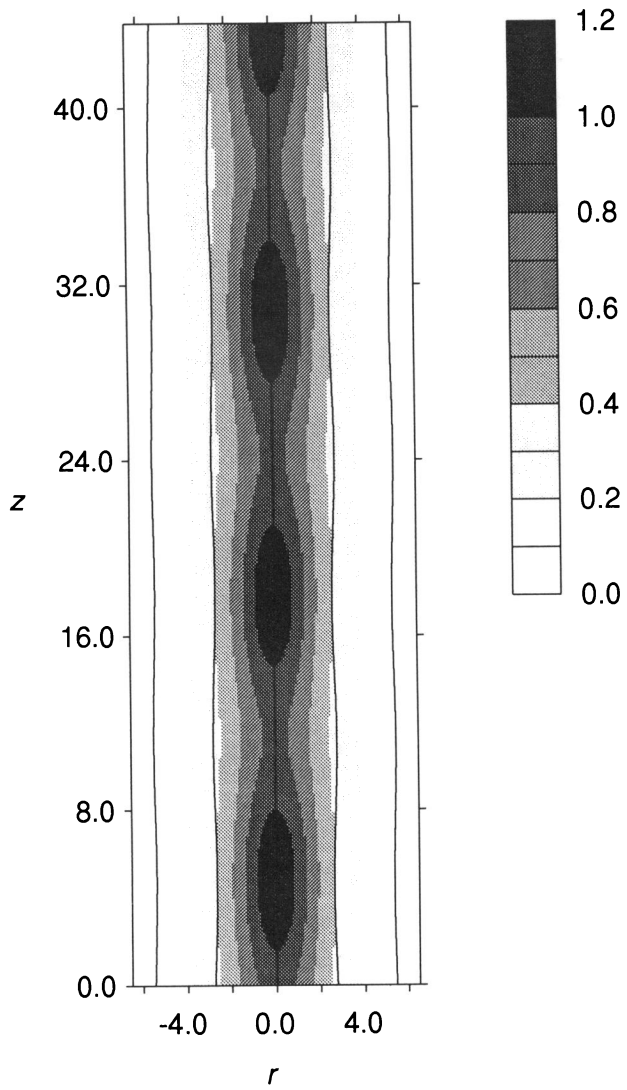

FIG. 1*a*

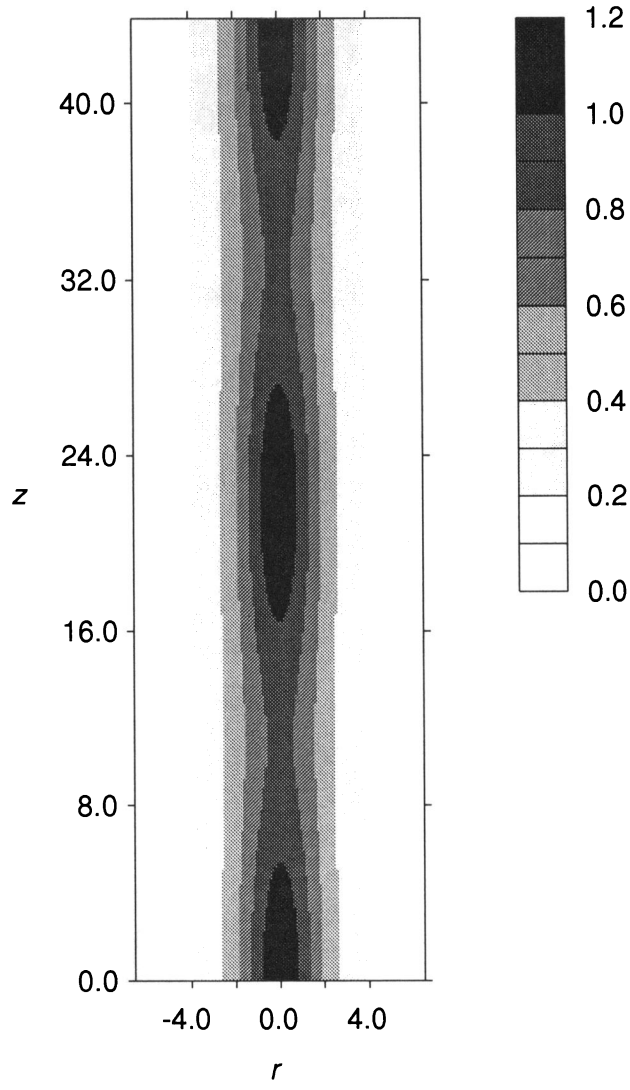

FIG. 1*b*

FIG. 1.—The column density distributions of the filamentary molecular clouds perturbed by the most unstable mode. The ordinate and abscissa are the linear dimensions in units of H across and along the filament axis, respectively. The eigenmode with the amplitude of $\rho_1/\rho_0 = 0.25$ at $r = 0$ is superposed on the equilibrium model. The left-hand panel (*a*) is for $\alpha = \beta = 0$ (nonmagnetized, nonrotating cloud) and the right-hand panel (*b*) for $\alpha = 1$ (magnetized) and $\beta = 0$ (nonrotating).

HANAWA et al. (see 404, L84)

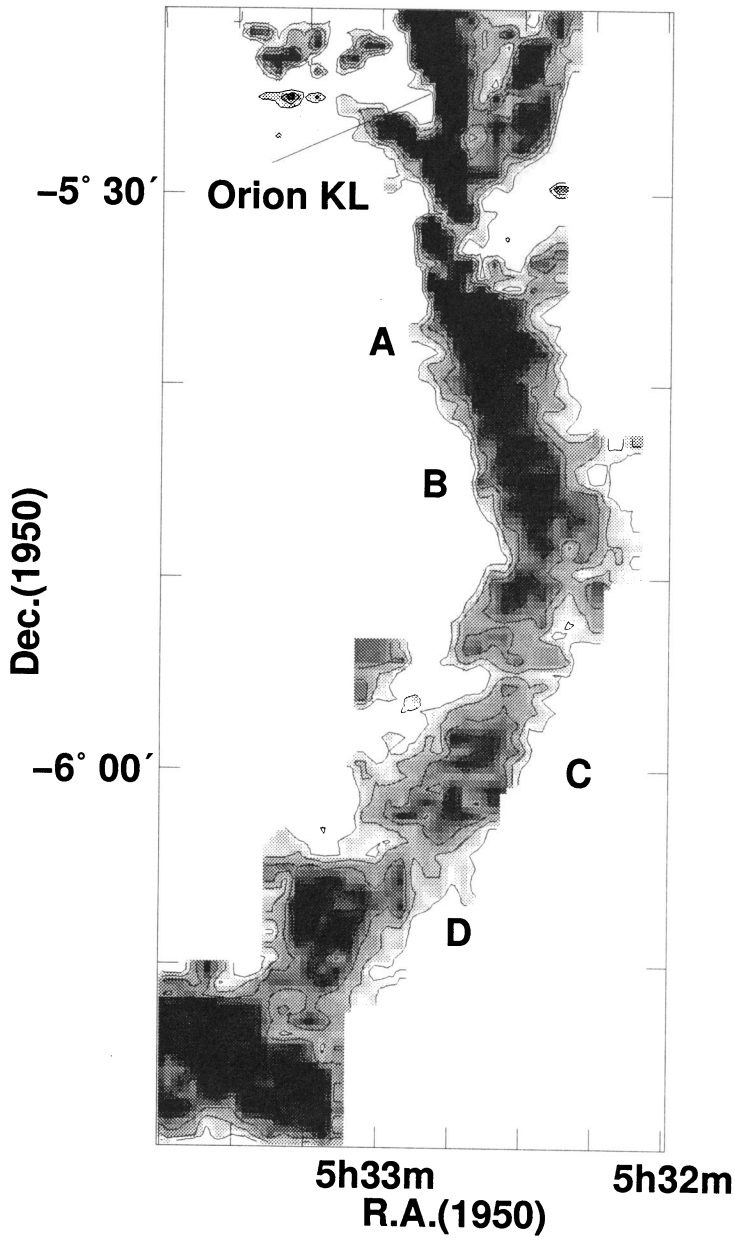

FIG. 2.—Peak intensity map of the ∫-shaped filament in Orion for the ^{13}CO ($J = 1–0$) emission line in the range of $V_{LSR} = 2.5–13.5$ km s^{-1}. The clumps labeled with letters are spaced more or less regularly with an interval of $\lambda = 1.4$ pc, while the effective diameter of the parent cloud is $d_{obs} = 0.69$ pc. The lowest level contour corresponds to $T_A^* = 4.0$ K (14 σ), and the level interval is $\Delta T_A^* = 0.8$ K (3 σ). Lower level contours are omitted to stress the structure of the relatively high density region. This figure is a close-up of Fig. 2 of Tatematsu et al. (1992).

HANAWA et al. (see 404, L84)

distribution (eq. [12]) assuming that the cloud is optically thin for this line. A least-squares fitting to the integrated ^{13}CO intensity map gives $d_{\rm FWHM}(^{13}{\rm CO}) = 0.69 \pm 0.19$ pc as an average for six strips between decl. $= -5°45'$ and $-6°12'$. We adopt the distance to the cloud of 450 pc.

The ratio of the brightness temperature $T(C^{18}O)/T(^{13}CO)$ averaged for 14 cores embedded in this region is 0.17 (Tatematsu et al. 1993). The closeness of this value to the abundance ratio $N(C^{18}O)/N(^{13}CO) \simeq 0.18$ expected from the terrestrial isotopic ratio suggests small optical thickness of the clumps for the ^{13}CO line. The optical thickness for the ^{13}CO line toward *IRAS* point sources in L1641, the southern part of the Orion A cloud, is between 0.2 and 0.7 (Morgan & Bally 1991). For Σ given by equation (12), an optical thickness less than 0.7 at $r = 0$ corresponds to $d_{\rm FWHM} < 5.1H$.

The apparent distance between the adjacent clumps projected on the sky, $\lambda_{\rm app}$, is typically 1.4 pc. Then we obtain

$$\frac{\lambda_{\rm app}}{d_{\rm FWHM}} = 2.03\left(\frac{\lambda_{\rm app}}{1.4\ {\rm pc}}\right)\left(\frac{d_{\rm FWHM}}{0.69\ {\rm pc}}\right)^{-1} = \left(\frac{\lambda}{d_{\rm FWHM}}\right)\sin i\ . \quad (14)$$

where i denotes the inclination angle of the filament axis from the line of sight. The inclination angle, i, is difficult to estimate and highly uncertain. Genzel & Stutzki (1989) estimated $i \sim 45°$ from the difference in the distances to the Orion Ia OB association and to the Orion Nebula and from the V-shaped feature in the cloud pointing its head toward the association. The value is, however, highly uncertain. If a filament is randomly oriented to the line of sight, the median value of the inclination angle is $i = 60°$. In the following we discuss the cases of $i = 30°$, 45°, 60°, and 75°. Substituting these values into equation (13) with $\theta = 0$, we obtain $\alpha + \beta = 0.10$, 0.77, 1.44, and 1.94 for $i = 30°$, 45°, 60°, and 75°, respectively. The effects of the magnetic field and rotation are evaluated to be negligibly small ($\alpha + \beta \ll 1$) only when $i < 30°$. In other words, the small apparent ratio of the distance to the diameter can be explained by either a very small inclination angle of 30° or the effects of rotation and magnetic fields.

Since the cloud must have contracted somewhat in the r-direction during fragmentation, the diameter of the parent cloud must have been larger than the present diameter $d_{\rm FWHM}$. Therefore, it is likely that the values of $\alpha + \beta$ are somewhat greater than the values obtained from the observed present-day diameter above, and the inclination angle i required for $\alpha + \beta = 0$ is even smaller than 30°. Also when the magnetic field is helical ($\theta \neq 0$) or when the optical depth of the emission line is less than $\tau < 0.7$, the inclination angle i required for $\alpha + \beta = 0$ is smaller than 30°. Thus the apparent small ratio of $\lambda_{\rm app}/d_{\rm FWHM}$ is in part due to magnetic fields and/or rotation except when the filamentary cloud is almost parallel to the line of sight.

The angular velocity of the rotation can be estimated independently from position-velocity diagrams of the emission line taken across the filamentary cloud. The velocity gradient across the major axis is evaluated to be 2–3 km s^{-1} pc^{-1} (Tatematsu et al. 1993). The velocity gradient across the filament is steeper than the velocity gradient along the filament although the velocity difference is larger for the latter. Therefore we can assume that the $\int$-shaped filament rotates mainly about its axis. We measured the velocity dispersion of the ^{13}CO profile to be 1.1 km s^{-1} toward the filament center. Because this is much greater than the thermal velocity of a CO molecule and considerably greater than the thermal velocity of an H_2 molecule expected in molecular clouds, we can regard this as an effective sound velocity, i.e., $c_s \simeq 1.1$ km s^{-1}. We also obtain $\Omega_c \simeq 1.0$–1.5×10^{-13} s^{-1} by fitting the position-velocity diagram of the same line to the model (see Appendix). Substituting these values into equation (8) we have $\beta \sin^2 i \simeq 0.3$–0.7. The term, $\sin^2 i$, denotes the projection effect of the rotation velocity. The obtained value of β is consistent with the results obtained from the separation of the clumps above if $i \geq 45°$. The effect of magnetic fields is thought to be appreciable if $i \geq 60°$.

On the basis of the above analysis, we can conclude that the magnetic field and/or rotation have played important roles in the fragmentation of the Orion A filamentary cloud. Comparison of the theory with observations for other molecular clouds would be invaluable in understanding the formation and evolution of filamentary molecular clouds, the common structure of the interstellar matter.

The authors thank M. Hayashi, T. Iwata, H. Mikami, Y. Murata, M. Nakano, N. Ohashi, K. Sunada, and H. Takaba for their collaboration in the stage of observation and their kind permission for the use of the data before publication. The present work is financially supported in part by the Grant-in-Aid for General Scientific Research (04640270) and that for Scientific Research on Priority Areas (Interstellar Matter and Its Evolution, 03249105) by the Ministry of Education, Science, and Culture, Japan.

APPENDIX

THEORETICAL EMISSION-LINE SPECTRUM

We compute the emission-line profile under the assumption that $\tau \ll 1$ for our filamentary gas cloud model:

$$I(v; r) = A\int_{-\infty}^{\infty}\rho(s)\exp\left\{-\frac{(v - v_0)^2}{2v_d^2}\right\}ds\ , \quad (A1)$$

where $v_d = (v_{\rm therm}^2 + v_{\rm turb}^2)^{1/2}$ is the velocity dispersion (thermal and turbulent) and

$$\rho(s) = \rho_c\left(1 + \frac{r^2 + s^2}{8H^2}\right)^{-2}\ , \quad (A2)$$

$$v_0(s) = \Omega_c r\left(1 + \frac{r^2 + s^2}{8H^2}\right)^{-1/2}\ . \quad (A3)$$

For simplicity we assumed that the cloud axis is perpendicular to the line of sight. Then the average velocity, $\langle v \rangle$, and the velocity dispersion, $\langle v^2 \rangle - \langle v \rangle^2$ are evaluated to be

$$\langle v \rangle \equiv \frac{\int vI(v)dv}{\int I(v)dv} = \frac{\int v_0 \rho \, ds}{\int \rho \, ds} = \frac{8}{3\pi} \frac{\Omega_c r}{\sqrt{1 + r^2/8H^2}}, \tag{A4}$$

$$\langle v^2 \rangle \equiv \frac{\int v^2 I(v)dv}{\int I(v)dv} = v_d^2 + \frac{\int v_0^2 \rho \, ds}{\int \rho \, ds} = v_d^2 + \frac{3}{4} \frac{\Omega_c^2 r^2}{1 + r^2/8H^2}. \tag{A5}$$

$$\langle v^2 \rangle - \langle v \rangle^2 = v_d^2 + \left(\frac{3}{4} - \frac{64}{9\pi^2} \right) \frac{8\Omega_c^2 H^2 r^2}{8H^2 + r^2}. \tag{A6}$$

Using equations (A4) and (A6) we can make a best-fit model to an observed molecular cloud.

REFERENCES

Bally, J. 1989, in Low Mass Star Formation and Pre Main Sequence Objects, ed. B. Reipurth (Garching: ESO), 1
Bally, J., Langer, W. D., Stark, A. A., & Wilson, R. W. 1987, ApJ, 312, L45
Castets, A., Duvert, G., Dutrey, A., Bally, J., Langer, W. D., & Wilson, R. W. 1990, A&A, 234, 469
Dutrey, A., Langer, W. D., Bally, J., Duvert, G., Castets, A., & Wilson, R. W. 1991, A&A, 247, L9
Genzel, R., & Stutzki, J. 1989, ARA&A, 27, 41
Heiles, C. 1987, in Interstellar Processes, ed. D. J. Hollenbach & H. A. Thronson (Dordrecht: Reidel), 171
Matsumoto, T., et al. 1993, in preparation
Morgan, J. A., & Bally, J. 1991, ApJ, 372, 505
Nagasawa, M. 1987, Progr. Theor. Phys., 77, 635
Nakamura, F., Hanawa, T., & Nakano, T. 1991, PASJ, 43, 685
———. 1992, PASJ, submitted
Ostriker, J. 1964, ApJ, 140, 1056
Stodółkiewicz, J. S. 1963, Acta Astron., 13, 30
Tatematsu, K., et al. 1993, ApJ, in press
Troland, T. H., Crutcher, R. M., & Kazés, I. 1986, ApJ, 304, L57
Uchida, Y., Fukui, Y., Minoshima, Y., Mizuno, A., Iwata, T., & Takaba, H. 1991, Nature, 349, 140
Vrba, F., Strom, S. E., & Strom, K. M. 1988, AJ, 96, 680

PLATE L9

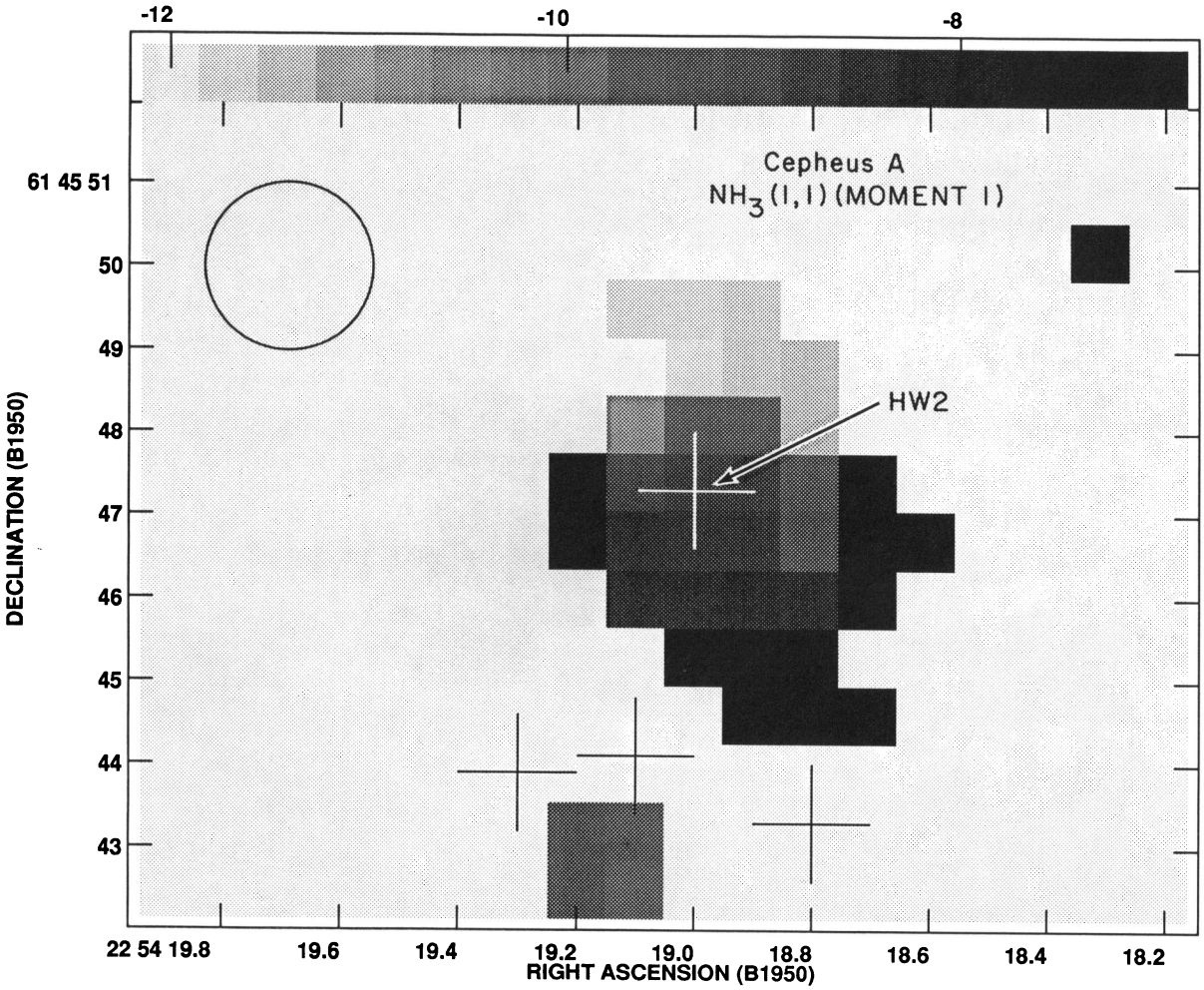

FIG. 3.—Gray-scale map of the second-order moment (velocity dispersion, σ) of the (1, 1) ammonia main hyperfine component toward HW 2. Other sources in the field (Hughes & Wouterloot 1984) are also indicated by crosses. To produce this map we have smoothed the individual channel maps to ~ 1.2 km s^{-1} of velocity resolution. Gray-scale ranges from 0 to 3 km s^{-1}. For Gaussian line profiles, the second-order moment corresponds to 0.85 times the HWHM line width.

TORRELLES, RODRÍGUEZ, CANTÓ, & HO (see 404, L76)